NACA

RESEARCH MEMORANDUM

TESTS IN THE AMES 40- BY 80-FOOT WIND TUNNEL OF AN AIRPLANE

CONFIGURATION WITH AN ASPECT RATIO 2 TRIANGULAR WING

AND AN ALL-MOVABLE HORIZONTAL TAIL -

LONGITUDINAL CHARACTERISTICS

By David Graham and David G. Koenig

Ames Aeronautical Laboratory
Moffett Field, Calif.

NATIONAL ADVISORY COMMITTEE
FOR AERONAUTICS

WASHINGTON
April 23, 1951

NATIONAL ADVISORY COMMITTEE FOR AERONAUTICS

RESEARCH MEMORANDUM

TESTS IN THE AMES 40- BY 80-FOOT WIND TUNNEL OF AN AIRPLANE

CONFIGURATION WITH AN ASPECT RATIO 2 TRIANGULAR WING

AND AN ALL-MOVABLE HORIZONTAL TAIL -

LONGITUDINAL CHARACTERISTICS

By David Graham and David G. Koenig

SUMMARY

An investigation has been made to determine the effect of an all-movable horizontal tail on the low-speed longitudinal characteristics of a triangular-wing airplane. The model consisted of a triangular wing of aspect ratio 2 in combination with a fuselage of fineness ratio 12.5; a thin, triangular, vertical tail; and a thin, unswept, all-movable horizontal tail. The wing had an NACA 0005 modified section and was equipped with partial-span, slotted, trailing-edge flaps. Tests were made with the horizontal tail at each of three vertical distances above the wing chord plane (0, 0.25, and 0.50 wing semispan) at one longitudinal distance behind the wing. The Reynolds number, based on the wing mean aerodynamic chord, was approximately 14.6×10^6 and the Mach number was 0.13.

The results of the tests of the model with the horizontal tail at each of the three vertical positions indicated that from a standpoint of longitudinal stability the most desirable position of those tested would be that in the extended wing-chord plane. Downwash studies show that destabilizing aerodynamic-center variations, obtained with the tail in either of the other two positions, are the result of the downwash variations with angle of attack. Further tests to investigate the trim characteristics of the model with the horizontal tail in the extended wing-chord plane indicated that gliding speeds at a given wing loading calculated for airplanes with and without a horizontal tail were, for comparable attitude and static margins, lower for the airplane with a horizontal tail.

INTRODUCTION

Theoretical and experimental studies show that an airplane with a low-aspect-ratio triangular wing would have desirable characteristics

for flight at moderate supersonic speeds. At low speeds, however, the triangular wing has several undesirable characteristics which if not over-come will limit its use. These undesirable characteristics include low lift-drag ratios and high angles of attack at maximum lift coefficients. Thus an airplane utilizing a triangular wing would have high sinking and landing speeds and abnormally high landing attitudes.

The foregoing considerations have neglected the problem of trim. Because of the characteristics of a triangular wing, trim can be obtained by the use of trailing-edge flaps (tailless airplane) as well as by other means such as a conventional horizontal tail. The tailless design, how-ever, further aggravates the low-speed problems associated with the use of a triangular wing. This is indicated by the data of reference 1 which show that the negative flap deflections required to trim the airplane increase both the drag and angle of attack at any given lift coefficient. In contrast, reference 1 also shows that, at a given lift coefficient, a reduction in both drag and angle of attack can be obtained by use of pos-itive flap deflections. Use of the trailing-edge flaps as a lift-producing device, however, would necessitate the use of a trimming device such as an all-movable horizontal tail.

In order to provide information on the low-speed characteristics of a triangular-wing airplane with a horizontal tail, an investigation was made in the Ames 40- by 80-foot wind tunnel. The model used in the investigation consisted of a thin, low-aspect-ratio, triangular wing with partial-span, slotted, trailing-edge flaps; a high-fineness-ratio fuselage; a thin vertical tail of triangular plan form; and a thin, unswept horizon-tal tail. The plan form of the horizontal tail was made identical, and the airfoil section similar, to that of the wing the characteristics of which, throughout the subsonic Mach number range, are reported in refer-ence 2. The choice of plan form was dictated by the following considera-tions: An all-movable horizontal tail was chosen from a consideration of stability and control. The use of a triangular, all-movable tail was eliminated because of geometry (i.e., large root chord), while the use of an all-movable, swept tail was eliminated as a result of a consideration of control moments. Hence, the unswept tail with a supersonic-type air-foil section was chosen. The horizontal tail was located at each of three vertical positions with respect to the wing-chord plane at a fixed longi-tudinal position of the tail. Reported herein are the longitudinal sta-bility and control characteristics of the various model configurations.

NOTATION

α free-stream angle of attack with reference to the wing-chord plane, degrees

b   wing span, feet

b_t horizontal-tail span, feet

c   wing chord, measured parallel to wing center line, feet

$\bar{c}$ mean aerodynamic chord of wing, measured parallel to wing center

$$\text{line} \left(\frac{\int_0^{b/2} c^2 \, dy}{\int_0^{b/2} c \, dy} \right), \text{ feet}$$

C_D drag coefficient $\left(\dfrac{D}{qS} \right)$

C_L lift coefficient $\left(\dfrac{L}{qS} \right)$

C_m pitching-moment coefficient $\left(\dfrac{M}{qS\bar{c}} \right)$

D   total drag, pounds

δ_f flap deflection, measured perpendicular to hinge line, degrees

ϵ local downwash angle, degrees

ϵ_{av} average effective downwash angle, degrees

i_t horizontal-tail incidence relative to the wing-chord plane, degrees

l_t distance from center of gravity to pivot line of horizontal tail, feet

L   total lift, pounds

L/D   lift-drag ratio

M   total pitching moment about the center of gravity, foot-pounds

q   free-stream dynamic pressure, pounds per square foot

q_l local dynamic pressure, pounds per square foot

S   wing area, square feet

S_t horizontal—tail area, square feet

V_g gliding speed, miles per hour

V_s sinking speed, feet per second

x longitudinal distance of the center of gravity aft of $\frac{\overline{c}}{4}$, feet

y lateral coordinate perpendicular to plane of symmetry, feet

z vertical coordinate perpendicular to wing chord plane, feet

APPARATUS

A three—view drawing of the model is shown in figure 1 and figure 2 is a photograph of the model in the Ames 40— by 80—foot wind tunnel. The pertinent dimensional data are presented in table I and figure 1.

The wing of the model had an aspect ratio of 2. The airfoil sections parallel to the model center line were modified NACA 0005 sections. The modification consisted of fairing the section from the 67—percent—chord station to the trailing edge by straight lines. Coordinates of the section are listed in table II. The wing was equipped with partial—span, constant—percent—chord, slotted flaps. Dimensions of the flaps are presented in figure 3(a) and the path of travel of the flap when it was deflected is shown in figure 3(b).

The fuselage was of circular cross section and had a fineness ratio of 12.5. Coordinates for the fuselage are presented in table III.

The vertical tail had a plan form that was similar to the semi—plan form of the wing. The airfoil sections parallel to the model center line were the modified NACA 0005 sections. The location of the vertical tail relative to the wing is shown in figure 1.

The all—movable horizontal tail was of unswept plan form and had a modified diamond section. The original diamond section of 5.6—percent thickness was modified by rounding the maximum—thickness ridge using a radius of curvature of 4.48 chord; the resulting section had a maximum thickness of 4.2—percent chord. The three positions of the horizontal tail used were, namely, a low, middle, and high position as shown in figure 1. The tail was pivoted about a line connecting the leading edges of the tip sections. In the low position, the horizontal tail was mounted on the fuselage with its pivot line in the extended chord plane of the wing. In the middle and high positions, the horizontal tail was mounted on the vertical tail with the pivot line located vertically at

approximately 25— and 50—percent wing semispan above the wing—chord plane, respectively. The longitudinal location was the same for all three tail positions. (See fig. 1.) The same tail—surface panels were used for the three positions. Consequently, the tail aspect ratio was larger with the tail at the low position than at the other two positions (4.4 and 4.0, respectively).

TESTS

Force and moment data were obtained for the model with the horizontal tail at each of the three positions and with the horizontal tail off. The tail was set at 0° and at —6° incidence at each of the three tail positions. All tests were made at zero sideslip. Flap deflections of 0° and 40° were used.

The tests were made through an angle—of—attack range of —1° to 26°, except for tests with the horizontal tail in the high position where the angle of attack was limited to a maximum of 18° due to structural limitations of the model.

Additional tests were made with the tail at the low position in order to determine the longitudinal trim characteristics of the model. Data were obtained for a range of horizontal—tail incidences from +1° through —10° for flap deflections of 0° and 40°, and for tail incidences of 0° and —10° for flap deflections of 10°, 20°, and 30°.

The Reynolds number of the tests was 14.6 million based on the mean aerodynamic chord of the wing. The dynamic pressure was approximately 25 pounds per square foot and the Mach number was 0.13.

RESULTS

The results of the tests with the horizontal tail at each of the three vertical positions and with the tail off are presented in figure 4. Figure 5 presents a comparison of the pitching—moment curves for the model with the tail at each of the three vertical positions, flaps undeflected, and tail incidence zero. In order to facilitate the discussion, the pitching—moment data are referred to center—of—gravity locations for which

a value of $\left(\dfrac{dC_m}{dC_L} \right)_{C_L=0}$ of —0.06 was obtained for each horizontal—tail

position when the trailing—edge flaps and the horizontal tail were

undeflected. These center—of—gravity positions are $0.426\bar{c}$, $0.464\bar{c}$, and $0.516\bar{c}$ for the low, middle, and high positions of the tail, respectively. The pitching—moment data for the tail—off configuration are referred to each of the three center—of—gravity positions for comparison with the data for the three tail—on configurations.

The foregoing data for the configurations with the undeflected flaps were used to determine the average effective downwash variation with angle of attack at each of the horizontal—tail positions. These down—wash data are shown in figure 6(a). The data were obtained by making the assumption that, at any given angle of incidence of the tail, when the moment of the tail—on configuration is equal to the moment of the tail—off configuration the tail does not contribute to the moment and hence the average angle of flow across the tail is zero. The average effective downwash at the tail, at the angle of attack where the tail—on and tail—off moment curves intersect, was then obtained by the rela—tion

$$\epsilon_{av} = \alpha + i_t$$

A linear variation of dC_m/di_t was assumed in order to obtain points of intersection for angles of incidence of the tail other than $0°$ and $-6°$.

Shown in figures 6(b) and 6(c) are the average effective downwash variations with angle of attack behind the wing without a fuselage and with undeflected flaps for values of $b_t/b = 0.63$ and 0.45, respectively. These were determined from a downwash survey in which directional pitot—static tubes were used to measure the downwash. Data are presented for the three positions corresponding to those used for the horizontal tail and at two intermediate positions. The average effective downwash was determined by use of the following relation:

$$\epsilon_{av} = \frac{2}{b_t} \int_0^{b_t/2} \epsilon \, dy$$

where ϵ was obtained at seven equally spaced intervals along the tail semispan. The values of q_l/q at the tail positions were not obtained during this survey. An indication of the values of q_l/q for the low tail position can be obtained, however, from the results of a survey of the downwash and wake in the extended chord plane of a similar wing (reference 3). These results indicate a variation of q_l/q from an average value of 0.8 at $\alpha = 0°$ to 1.0 at $\alpha = 14°$ and above.

The results of additional tests made to determine the trim charac—teristics of the model with the tail in the low position are shown in figure 7. It will be noted that the stability and the trim lift coef—ficient (particularly with $-10°$ tail incidence) of the model varied

irregularly with increasing flap deflection. The source of this effect
could not be determined from the available data. The lift and drag char-
acteristics of the trimmed configuration, determined from figure 7, are
shown in figure 8. Curves of constant gliding and sinking speeds, com-
puted for a wing loading of 30 pounds per square foot, are included in
this figure. Also shown in figure 8 are the low-speed lift and drag
characteristics determined from tests in the Ames 40- by 80-foot wind
tunnel (reference 4) of a tailless airplane having a triangular wing of
nearly the same aspect ratio as that of the present configuration (2.3
compared to 2.0). The characteristics of the trimmed tailless airplane
were derived from the data shown in figure 9 by interpolation for a
series of flap deflections. A static margin of $0.06\overline{c}$ was also assumed
for the data of figure 8.

The data were corrected for wind-tunnel-wall effects and support-
strut interference.

DISCUSSION

Effects of Vertical Location of the Horizontal Tail

The effect of horizontal-tail location on the static longitudinal
stability of the model is indicated by the data of figure 5. The varia-
tion of pitching-moment coefficient with lift coefficient is shown for
each of the three horizontal-tail configurations with zero trailing-
edge-flap deflection and zero incidence of the tail. These curves are
representative of the general trend of the pitching-moment variations
for the combinations of trailing-edge-flap deflections and tail incidences
tested for each of the tail positions. It can be seen that only the con-
figuration with the tail in the low position had a pitching-moment varia-
tion that was stable throughout the lift-coefficient range. With the
tail in the middle position, the model was stable through the low lift-
coefficient range, became unstable through the middle of the lift-
coefficient range ($0.23\overline{c}$ forward shift of the aerodynamic center), and
then returned to marginal stability at the highest lift coefficients
obtained during the present tests. With the tail in the high position,
the model was stable through the low lift-coefficient range, then became
and remained unstable ($0.47\overline{c}$ forward shift of the aerodynamic center)
through the remainder of the lift range of these tests.

These changes in stability were the result of the manner in which
the downwash behind the wing varied with angle of attack, as can be seen
by a comparison of the pitching-moment curves of figure 5 with the corre-
sponding downwash curves of figure 6(a). These downwash variations are
substantiated by the survey downwash curves, shown in figure 6(b), since

they have nearly the same shape as the corresponding curves determined from the force—test data. It can be seen that the changes in stability are related to changes in $d\epsilon_{av}/d\alpha$. For instance, with the tail in the low position, the stability of the model began to increase in the angle—of—attack range above 5° when $d\epsilon_{av}/d\alpha$ began to decrease. With the tail in either the middle or the high positions, the instability of the model occurred when $d\epsilon_{av}/d\alpha$ increased to values[1] greater than 0.8 and 0.7 for the two positions, respectively. At an angle of attack of approximately 20°, $d\epsilon_{av}/d\alpha$ for the model with the tail in the middle position decreased to values below 0.8 but, due to a decrease in the stability of the tail—off configuration (see fig. 4(b)) at the higher angles of attack, the stability of the complete model was only marginal.

These downwash variations are believed to be a result of the separation—vortex type of flow which has been shown to exist on thin tri-angular wings (references 3 and 4). Figure 10 shows that, as the angle of attack is increased, the vortices increase in strength and move inward and, relative to any given horizontal—tail position, move upward. It is evident that these changes in the vortex pattern will account qualita-tively for the changes in $d\epsilon_{av}/d\alpha$ with angle of attack for the various tail positions.

In order to determine what the stability characteristics of the model might be with the tail at positions between the low and middle pos—ition or with a tail of smaller span than that tested, the data obtained from the downwash survey (figs. 6(b) and 6(c)) were analyzed further. The survey data should be suitable in this respect since, as noted previ-ously, for the three positions investigated, the survey downwash curves of figure 6(b) have nearly the same shape as the corresponding curves determined from the force—test data. From the analysis, it was found that the downwash variation at a position halfway between the low and middle positions would have a variation similar to that which occurred at the middle tail position but with more gradual change in $d\epsilon_{av}/d\alpha$. This can be noted in figure 6(b) in which the downwash variations at two intermediate positions $\left(\dfrac{z}{b/2} = 0.13 \text{ and } 0.38\right)$ are compared with those for the three other positions. Since there are no large destabilizing variations in $d\epsilon_{av}/d\alpha$ for a height of $\dfrac{z}{b/2} = 0.13$, it appears very likely that the use of tail positions at or below this height would be satisfactory from a low—speed—stability standpoint. As indicated by the downwash variation at $\dfrac{z}{b/2} = 0.38$, a large destabilizing movement of

---

[1] The values of $d\epsilon_{av}/d\alpha$ which result in instabilities of the model are a function of the moment—center location.

the aerodynamic center can be expected for tail positions intermediate to the middle and high positions. As shown in figure 6(c), a reduction in the span of the horizontal tail to a value of $b_t/b = 0.45$ does not greatly alter the general variation of the downwash with angle of attack for the vertical positions shown. Therefore, the conclusions drawn with regard to the effect of tail height or stability for the tail span tested can be considered applicable to tails of lesser span, at least to the extent considered in figure 6(c). It is of interest to note that, for either tail span, as the tail height decreased, so did the angle-of-attack range through which the value of $d\epsilon_{av}/d\alpha$ produced a destabilizing effect, and hence a decrease should also occur in the lift-coefficient range through which the pitching moment due to the tail has an unstable variation.

Trim Characteristics

As indicated by the trim characteristics presented in figure 8, the triangular-wing airplane with a horizontal tail should have generally better trim lift and drag characteristics than a similar airplane without a tail. As might be expected, higher lift coefficients for a given angle of attack can be obtained when a tail is used. For example, at an angle of attack of 16° the following comparison of lift coefficient for trim and gliding and sinking speeds are obtained:

CONFIGURATION	C_L	$*V_g$ (mph)	$*V_s$ (fps)
Tailless airplane	0.59	140	45
Airplane with tail, $\delta_f = 40°$	1.04	104	50

$*W/S = 30$ pounds per square foot.

It can be seen that, by use of trailing-edge flaps as lift-producing devices and an all-movable horizontal tail as a longitudinal stabilizer and control, a 26-percent lower gliding speed can be realized. The sinking speed, however, is still quite high.

The results shown in the foregoing table are based on an assumed static margin of 6 percent and a landing attitude of 16° which may have unduly penalized the tailless model. Therefore, other conditions should be considered for a comparison of the trimmed characteristics of the two models. The following table lists values of gliding and sinking speeds for the two models with a 3-percent static margin for two angles of

attack:

CONFIGURATION	C_L	$*V_g$ (mph)	$*V_s$ (fps)
Tailless, $\alpha = 16°$	0.64	134	43
Tailless, $\alpha = 24°$	.96	107	56
Airplane with tail, $\delta_f = 40°$, $\alpha = 16°$	1.06	102	49
Airplane with tail, $\delta_f = 40°$, $\alpha = 24°$	1.44	86	54

$*W/S = 30$ pounds per square foot.

These results show that if low static margins are acceptable and if no ground-angle limitation is placed on the tailless model, then there is little to chose between the two from low-speed considerations. Possible weight and drag penalties incurred by use of a horizontal tail may therefore dictate against its use. Finally, however, it should be noted that there is no certainty that optimum flaps were tested on the model with a tail; hence the possibility remains, for this model, of making substantial improvements through refinements in flap design.

The values quoted in the foregoing tables are not completely indicative of the landing characteristics, since ground effects were not taken into account. As shown in reference 5, very large ground effects can be expected for a low-aspect-ratio triangular wing. Sizable increases in both C_L and L/D at a given angle of attack were obtained when the wing was within a semispan of the ground. These increases in C_L and L/D would result in decreases in both the gliding and sinking speeds of both configurations. No estimation of the ground effect on the effectiveness of the slotted-trailing-edge flap can be made at this time but, as shown in reference 5, there is a slight increase in flap effectiveness of split flaps on a triangular wing in the presence of the ground.

An estimate of the tail incidence necessary to trim the airplane, when near the ground, was made in order to determine whether the required incidences would be excessive. The change in pitching moment obtained for the triangular wing with split flaps in the presence of the ground (reference 5) was assumed to apply to the wing with the slotted flaps. In addition, in order to be conservative, it was assumed that the downwash at the tail is entirely eliminated by the presence of the ground. Based on these assumptions and a 6-percent static margin, the required incidence of the tail would be −22° when the wing is at an angle of 16° with flaps deflected 40° and at a distance of one semispan above the ground. This incidence is not considered to be excessive. The angle of attack of the tail relative to the local stream would be −6°.

Another point worthy of note is that, although the theoretical induced drag of a wing with aspect ratio 2 is over 15 percent greater than the induced drag of an aspect ratio 2.3 wing, the total drag at trim lift coefficients above 0.4 of the configuration with the all-movable horizontal tail and aspect ratio 2 wing is less than the total drag of the tailless airplane with the aspect ratio 2.3 wing, again referring to the cases where a 6-percent static margin was chosen.

CONCLUDING REMARKS

The results of the investigation of the model with the horizontal tail at each of the three vertical positions indicated that from a standpoint of longitudinal stability the most desirable position of those tested is that in the extended wing-chord plane. With the tail in this position, the model had a stable aerodynamic-center variation throughout the lift range; whereas the model with the tail in either of the two positions above the chord plane had large destabilizing variations through part or all of the lift range. Downwash studies show the destabilizing variations of the aerodynamic center for the model with the tail in either of the two positions above the extended wing-chord plane are the result of large increases in the rate of change of downwash with angle of attack through a part of the angle-of-attack range. The downwash survey indicates that the use of a horizontal tail at positions slightly (order of 0.1 b/2) above the extended wing-chord plane would also be satisfactory.

Gliding speeds at a given wing loading calculated for the airplane with and without a horizontal tail were, for comparable attitude and static margins, lower for the airplane with a horizontal tail. As the allowable attitude was reduced and/or minimum static margin increased the difference in gliding speeds became greater.

National Advisory Committee for Aeronautics,
    Ames Aeronautical Laboratory,
        Moffett Field, Calif.

REFERENCES

1. Graham, David: Chordwise and Spanwise Loadings Measured at Low Speeds on a Large Triangular Wing Having an Aspect Ratio of 2 and a Thin, Subsonic-Type Airfoil Section. NACA RM A50A04a, 1950.

2. Johnson, Ben H., Jr.: Investigation of a Thin Wing of Aspect Ratio 4
    in the Ames 12-Foot Pressure Wind Tunnel. I — Characteristics of a
    Plain Wing. NACA RM A8D07, 1948.

3. Anderson, Adrien E.: An Investigation at Low Speed of a Large-Scale
    Triangular Wing of Aspect Ratio Two. — II. The Effect of Airfoil
    Section Modifications and the Determination of the Wake Downwash.
    NACA RM A7H28, 1947.

4. Anderson, Adrien E.: Chordwise and Spanwise Loadings Measured at
    Low Speed on Large Triangular Wings. NACA RM A9B17, 1949.

5. Rose, Leonard M.: Low-Speed Investigation of a Small Triangular
    Wing of Aspect Ratio 2.0. I — The Effect of Combination with a
    Body of Revolution and Height Above a Ground Plane. NACA RM A7K03,
    1948.

TABLE I.— GEOMETRIC DATA OF MODEL

Wing

    Area, square feet 312.5
    Span, feet 25.00
    Mean aerodynamic chord, feet 16.67
    Aspect ratio 2
    Taper ratio 0

Fuselage

    Length, feet 56.16
    Maximum diameter, feet 4.49
    Fineness ratio 12.5

Vertical tail

    Exposed area, feet 52.53
    Aspect ratio 1
    Taper ratio 0

Trailing—edge flaps

    Area (total movable), square feet 37.44
    Chord 0.2084c

Horizontal tail

    Low position

        $\dfrac{S_t}{S}$ 0.246

        $\dfrac{b_t}{b}$ 0.738

        $\dfrac{l_t}{c}$ (c.g. at $0.426\overline{c}$) 1.161

        Aspect ratio 4.4
        Taper ratio 0.46

    Middle position

        $\dfrac{S_t}{S}$ 0.200
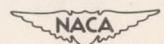
        $\dfrac{b_t}{b}$ 0.632

TABLE I.— CONCLUDED

Horizontal tail

  Middle position

  $\dfrac{l_t}{c}$ (c.g. at $0.464\overline{c}$) 1.123

  Aspect ratio 4.0
  Taper ratio 0.50

  High position

  $\dfrac{S_t}{S}$ 0.200

  $\dfrac{b_t}{b}$ 0.632

  $\dfrac{l_t}{c}$ (c.g. at $0.516\overline{c}$) 1.071

  Aspect ratio 4.0
  Taper ratio 0.50
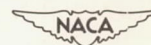
NACA

TABLE II.— COORDINATES OF THE NACA 0005
(MODIFIED) SECTION

Station (percent chord)	Ordinate (percent chord)
0	0
1.25	.789
2.50	1.089
5.00	1.481
7.50	1.750
10.00	1.951
15.00	2.228
20.00	2.391
25.00	2.476
30.00	2.501
40.00	2.419
50.00	2.206
60.00	1.902
67.00	1.650
70.00	1.500
80.00	1.000
90.00	.500
100.00	0
L.E. radius: 0.275—percent chord	
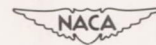
TABLE III.— BODY COORDINATES

[Stations and radii are in percent
of the total length.]

Station		Radius
0	100.00	0
.625	99.375	.26
1.25	98.75	.42
2.50	97.50	.70
5.00	95.00	1.15
7.50	92.50	1.54
10.00	90.00	1.86
15.00	85.00	2.41
20.00	80.00	2.86
25.00	75.00	3.22
30.00	70.00	3.51
35.00	65.00	3.73
40.00	60.00	3.88
45.00	55.00	3.97
50.00	– – –	4.00

NACA

Dimensions shown in feet
unless otherwise noted

c.g. Location

Tail position	x
Low	2.93
Middle	3.57
High	4.43

9.46°

12.50

9.22

7.91

63.43°

$\bar{c} = 16.67$

$\frac{\bar{c}}{4}$

4.17

8.70

12.50

21.04°

Pivot line

25.00

22.30

23.91

26.24

17.92

63.43°

8.96

x

6.33

3.17

56.16

NACA

Figure 1. - Geometric details of the model.
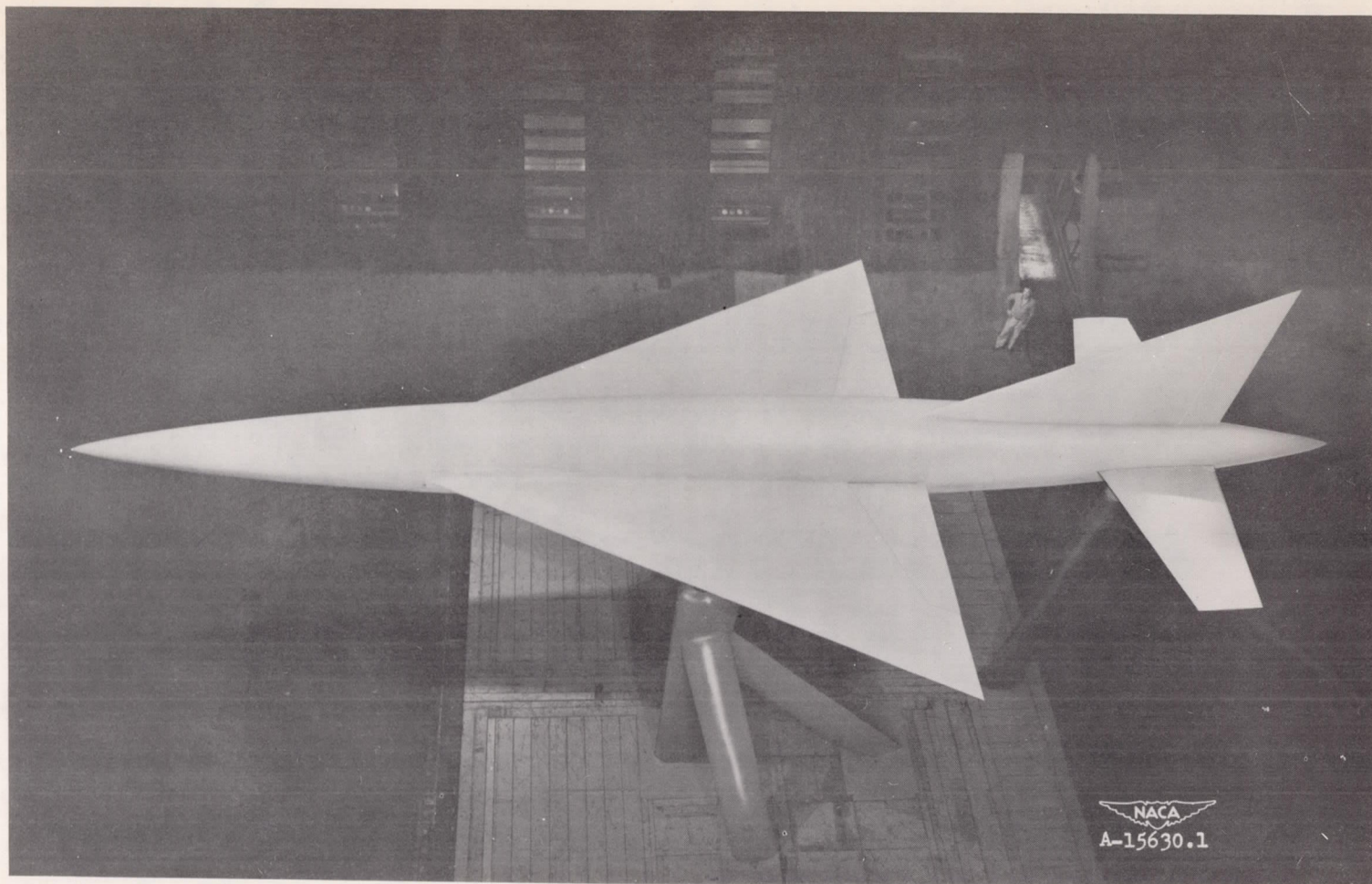
Figure 2.— The model as mounted in the Ames 40— by 80—foot wind tunnel. Horizontal tail in low position.

Edge of slot lip

4.30

Wing chord line

.55 .49

.76

.60

.52 R

Flap hinge point

Section shown parallel
to model center line.

20.84 from T.E. of wing
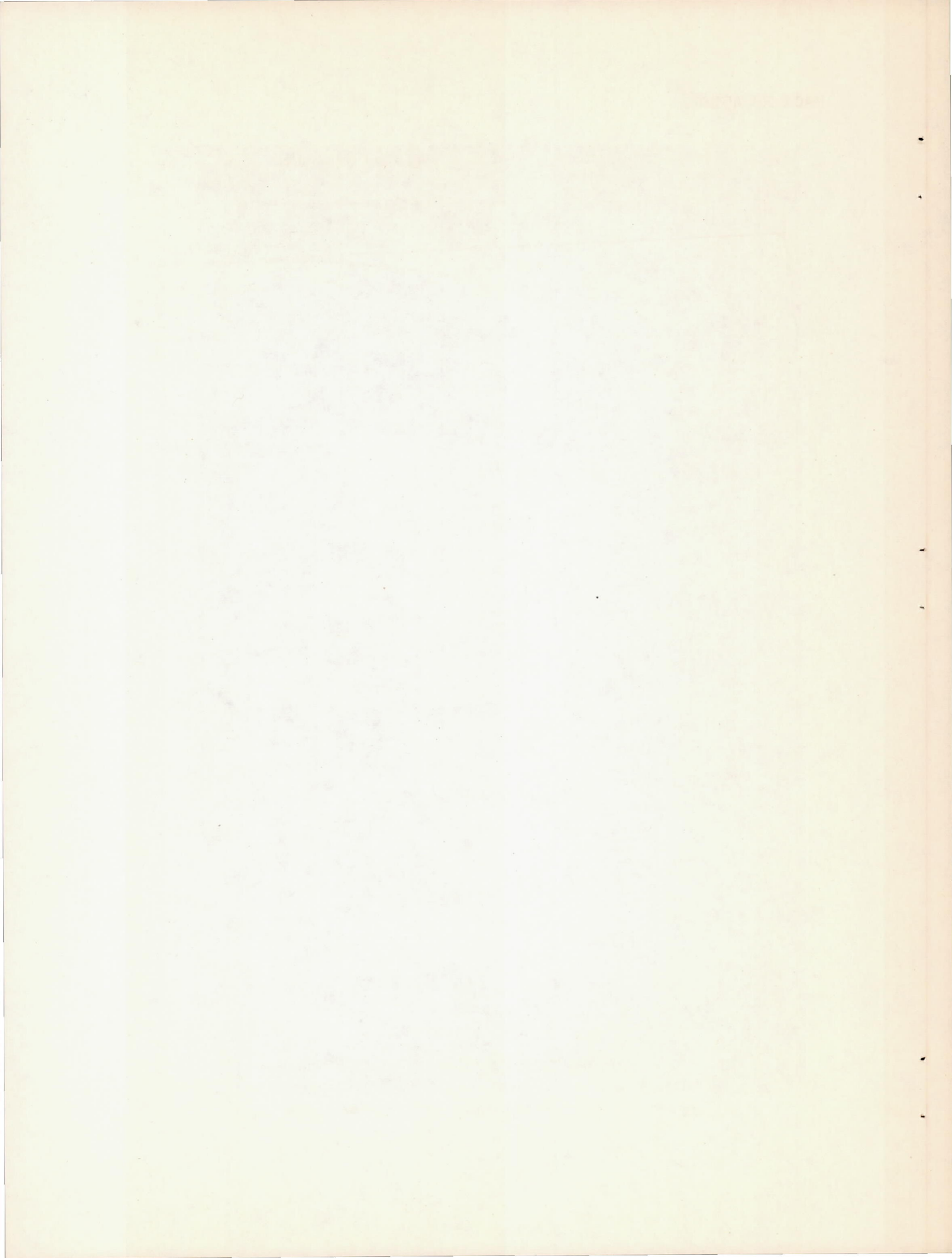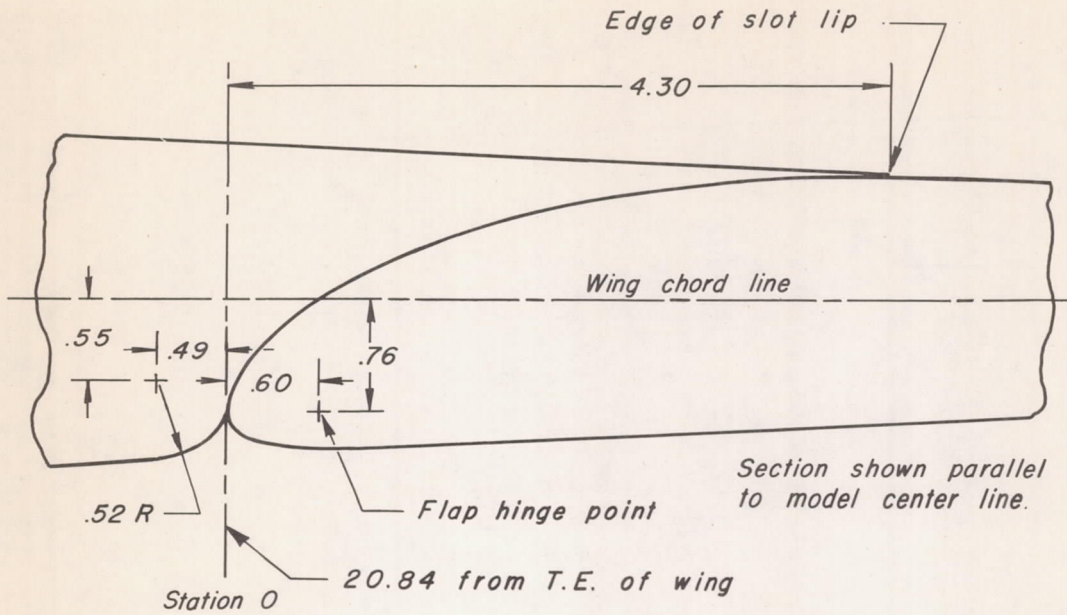
Station 0

Flap coordinates		
Station	Upper surface	Lower surface
0	−0.77	−0.77
.10	− .49	− .91
.20	− .36	− .96
.40	− .16	− .99
.60	− .01	−1.00
1.20	.31	− .99
1.80	.52	− .96
2.40	.66	− .92
3.00	.76	− .89
3.60	.80	− .86
4.20	.81	− .83
5.00	.80	− .80
10.00	.54	− .54
15.00	.29	− .29
20.84	0	0
Center of L.E. arc		
.15	−.77	
L.E. radius: 0.15		
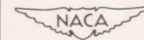
Dimensions shown in percent wing chord.

(a) Geometric details of flap.

Figure 3.- Details of the slotted, trailing-edge flap.

Edge of slot lip

Percent wing chord

40°

30°

δ_f, 0°   10°   20°

Percent wing chord

−4.0   −3.2   −2.4   −1.6   −.8   0   .8   1.6

0

.8

1.6

2.4
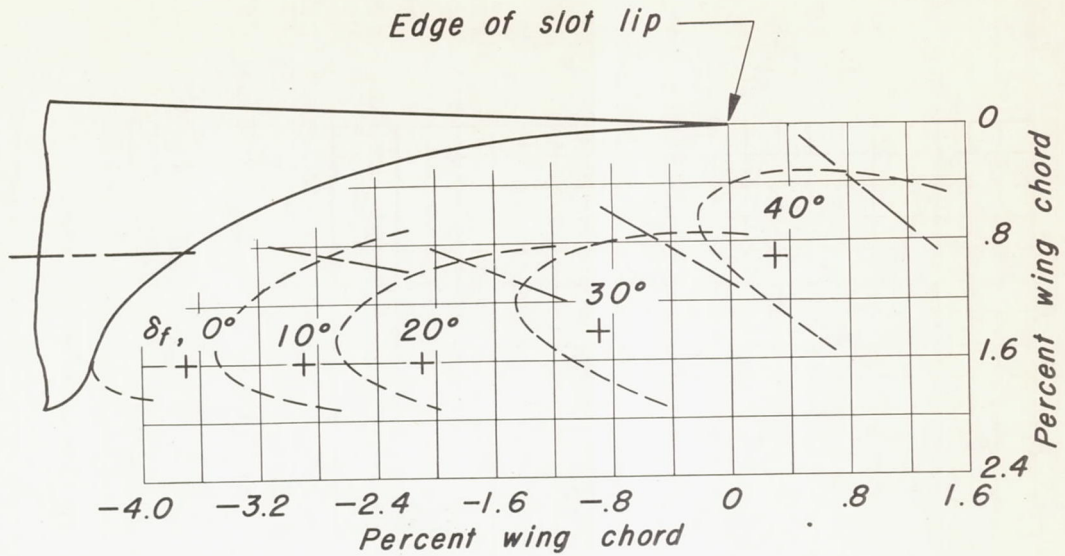
Section parallel to model center line.

+ Point at which flap hinge line intersects section plane. Flap deflection, δ_f, is measured perpendicular to flap hinge line.

Model center line

2.50 feet

This point on hinge line moves parallel to model center line.

NACA

T.E.
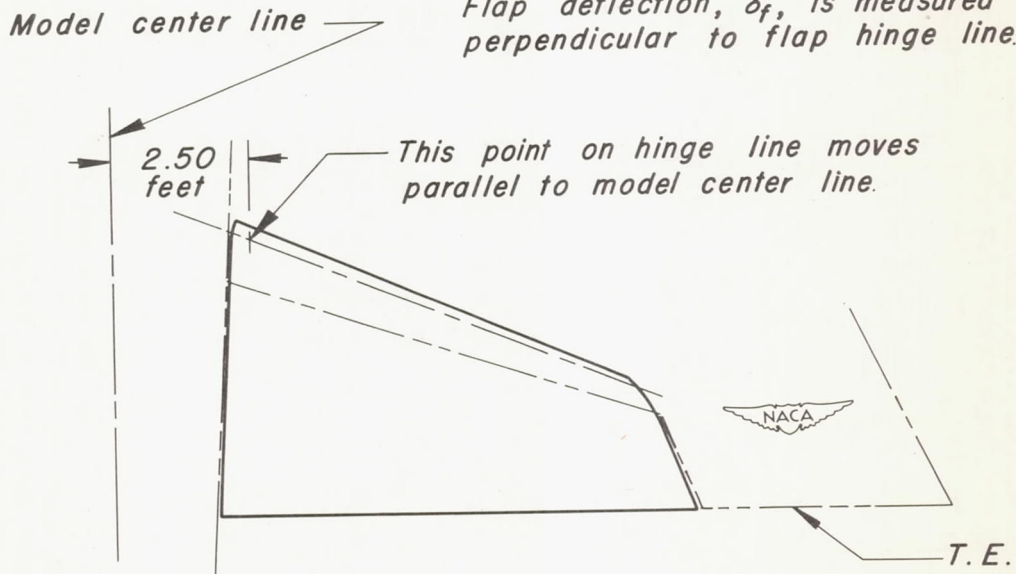
(b) Path of flap travel.

Figure 3.- Concluded.

δ_f, deg	i_t, deg
0	0
0	-6
0	tail off
40	0
40	-6
40	tail off

Lift coefficient, C_L

Angle of attack, α, deg

Pitching-moment coefficient, C_m

Drag coefficient, C_D
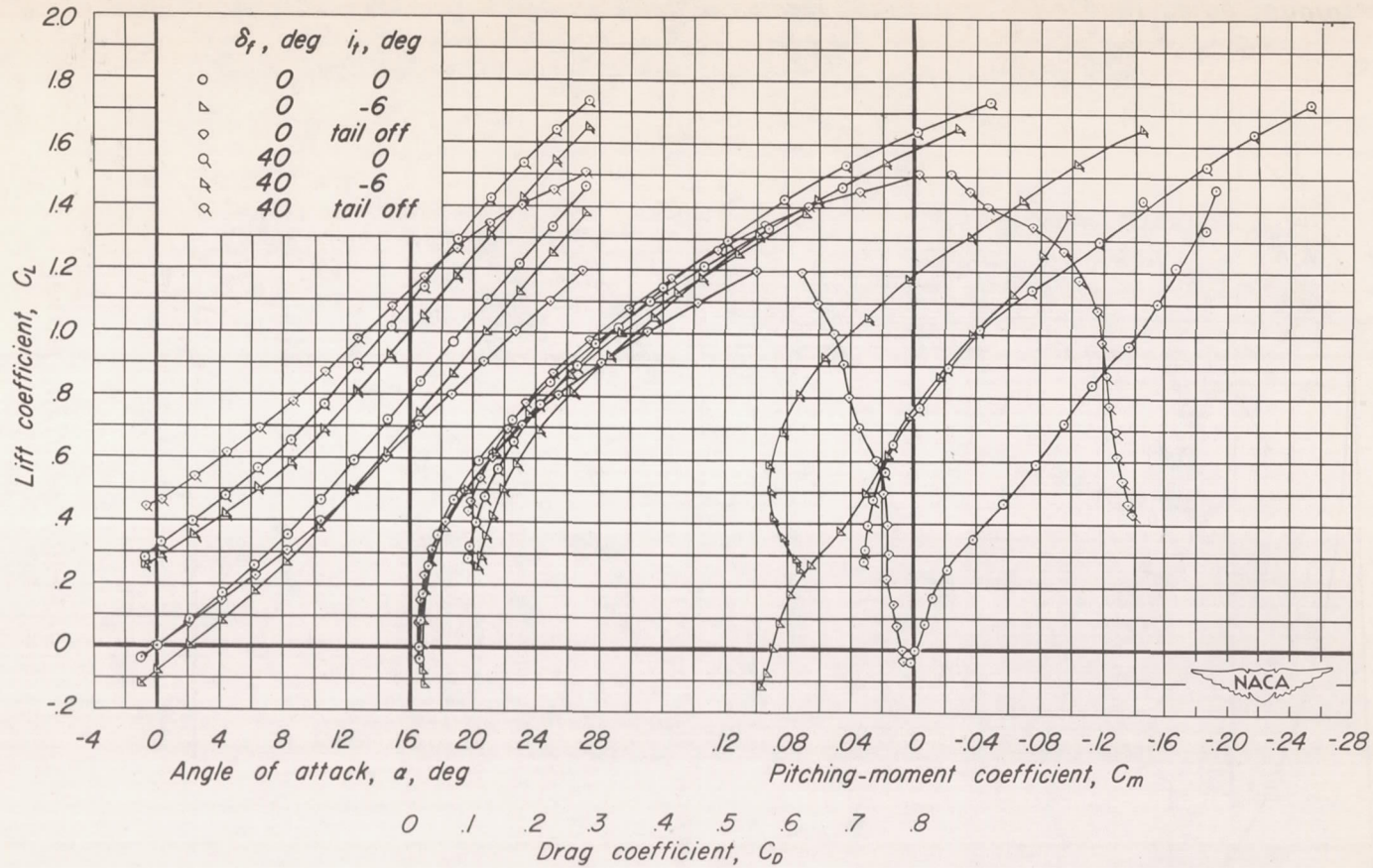
(a) Horizontal tail in low position. $\frac{z}{b/2}$, 0; c.g., 0.426 $\bar{c}$.

Figure 4.- Effect of horizontal-tail location on the aerodynamic characteristics of the model.
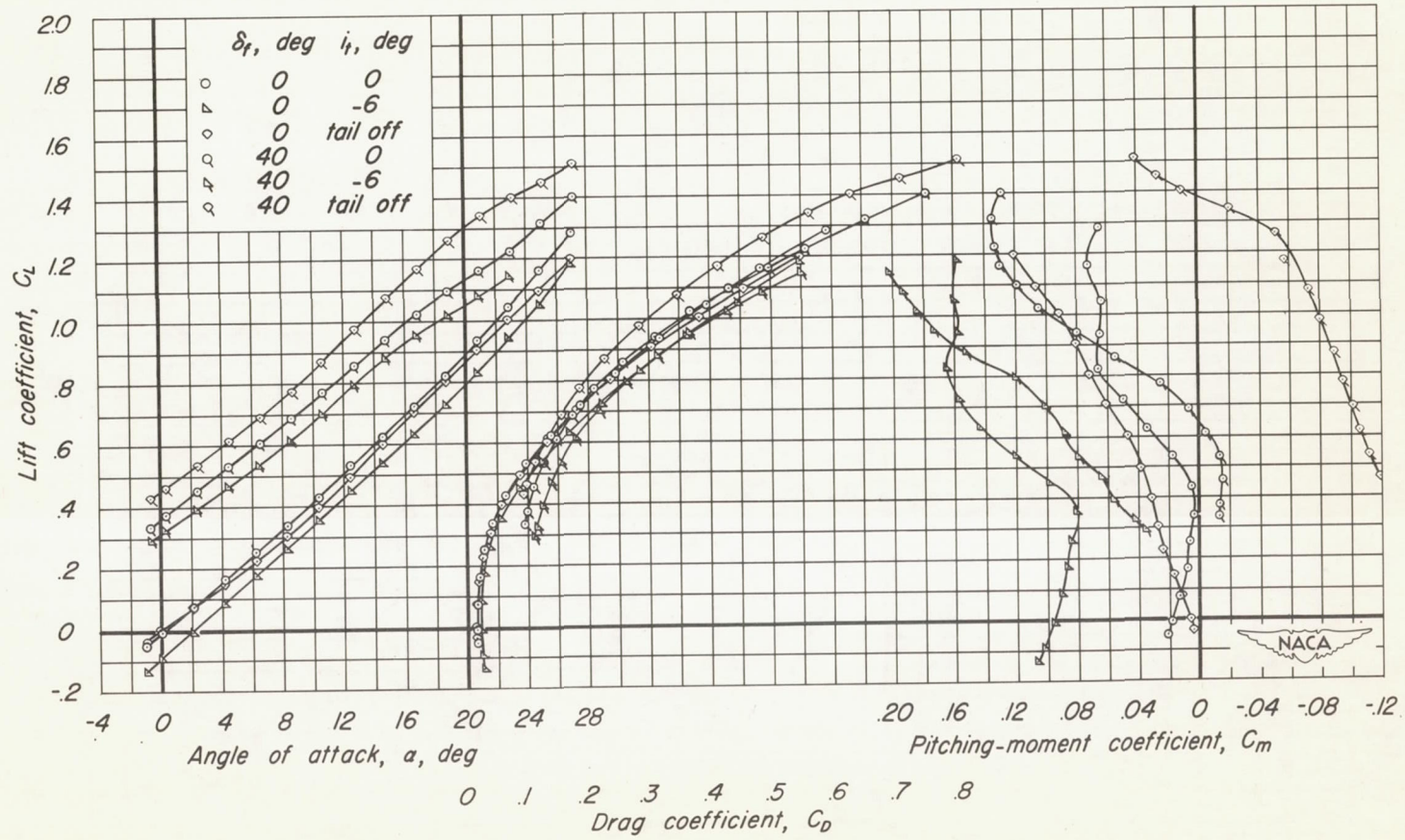
(b) Horizontal tail in middle position. $\frac{z}{b/2}$, 0.25; c.g., 0.464 $\bar{c}$.

Figure 4.- Continued.
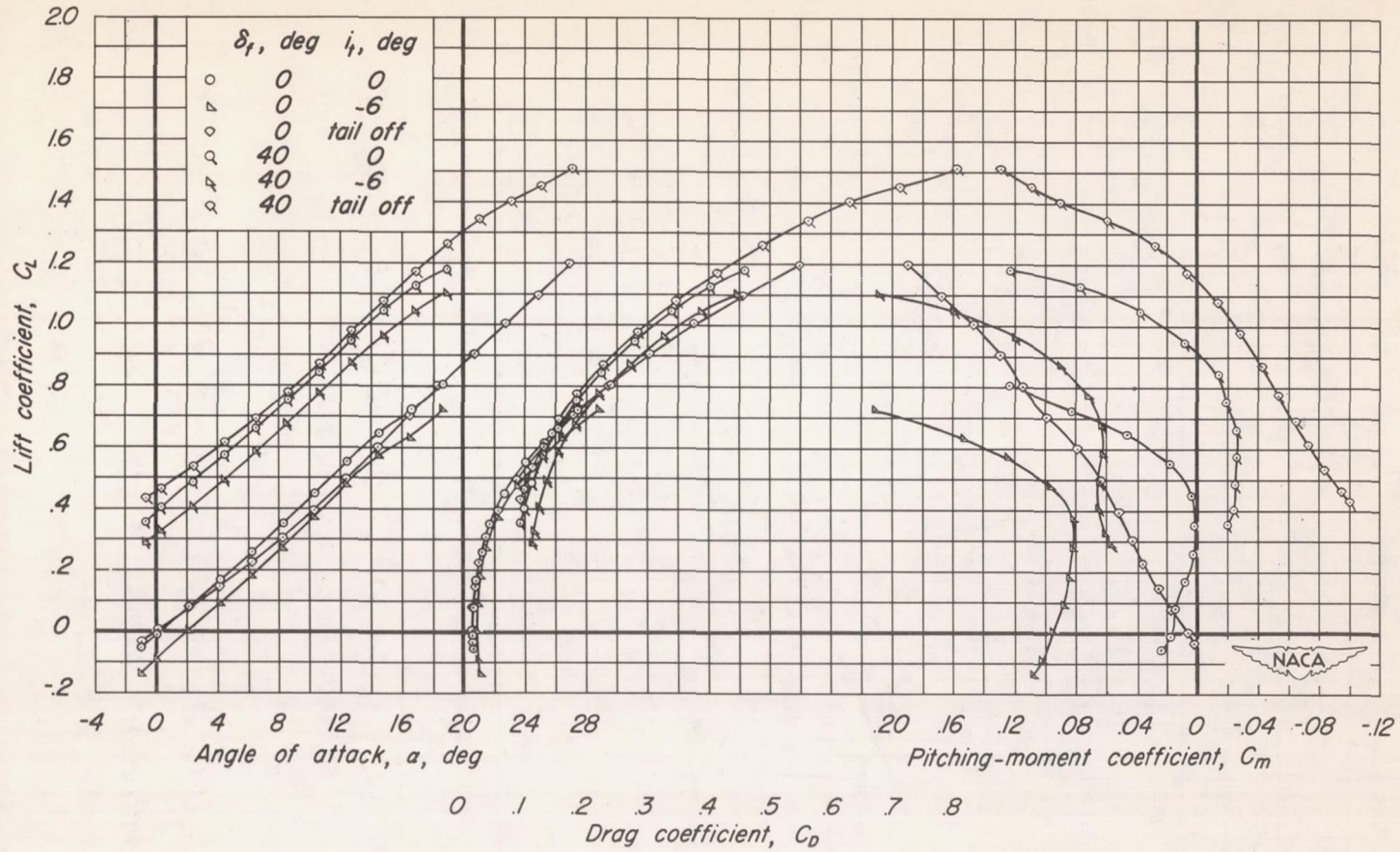
(c) Horizontal tail in high position. $\frac{z}{b/2}$, 0.50; c.g., 0.516 $\bar{c}$.

Figure 4.- Concluded.
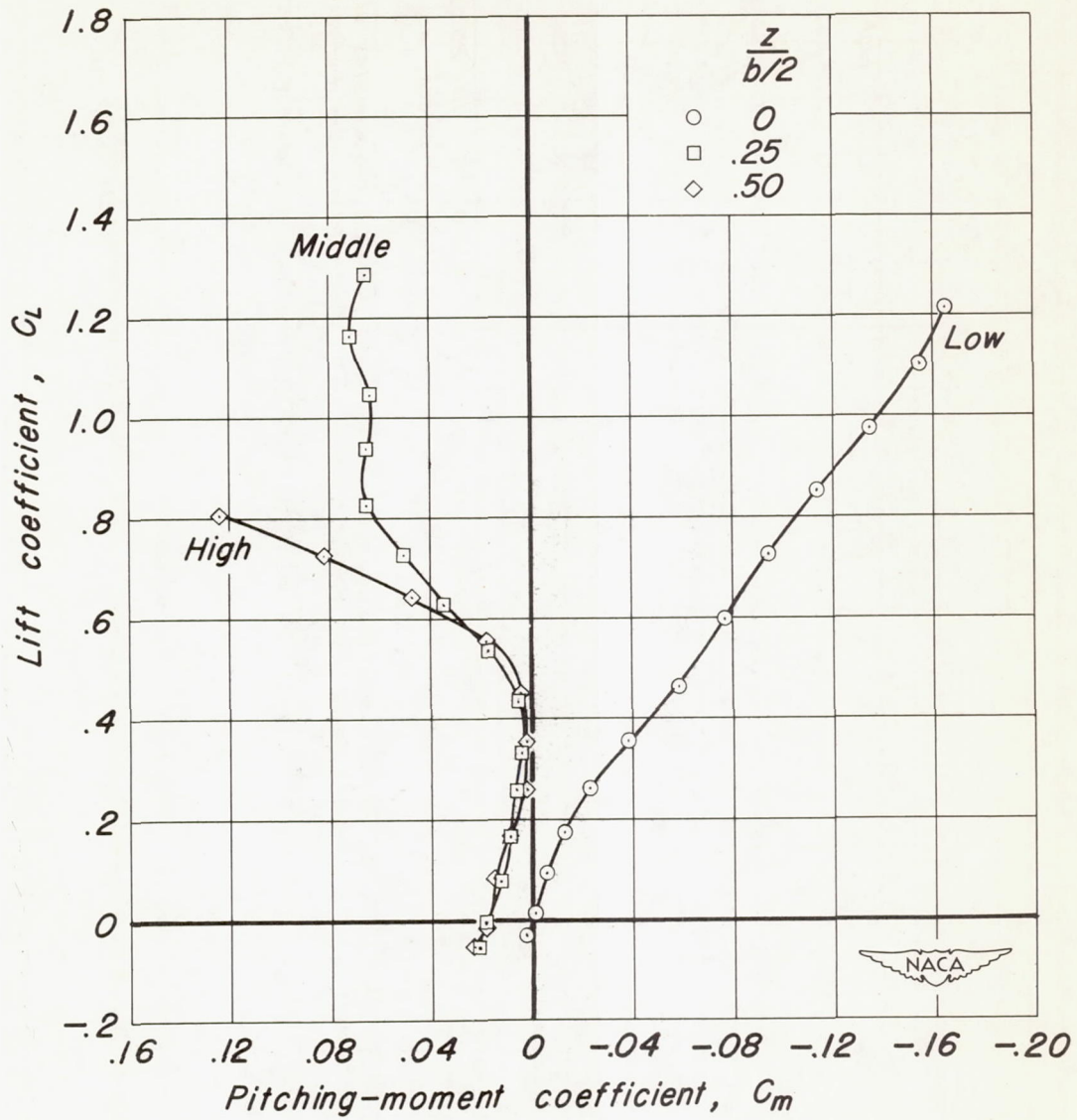
Figure 5.- Effect of vertical location of the horizontal tail on the static longitudinal stability of the model. $\left(\dfrac{dC_m}{dC_L}\right)_{C_L=0}$, -0.06; δ_f, 0°; i_t, 0°.
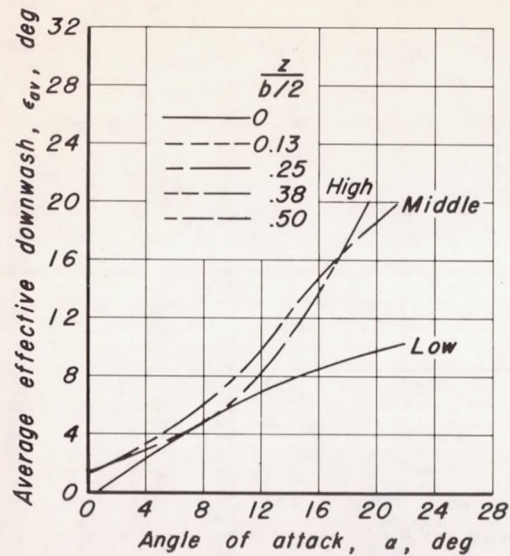
(a) Downwash characteristics of complete model, obtained from force tests.
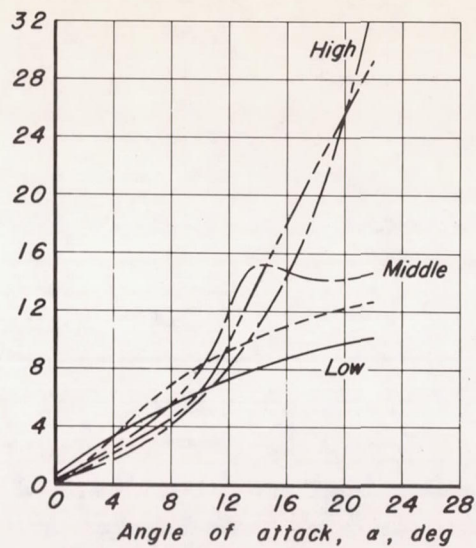
(b) Downwash characteristics of wing alone, obtained from downwash survey. b_t/b, 0.63.
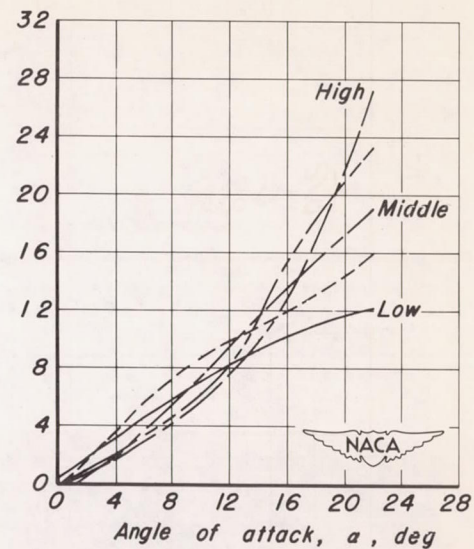
(c) Downwash characteristics of wing alone, obtained from downwash survey. b_t/b, 0.45.

Figure 6.- Variation of average effective downwash angle with angle of attack. δ_f, 0°.
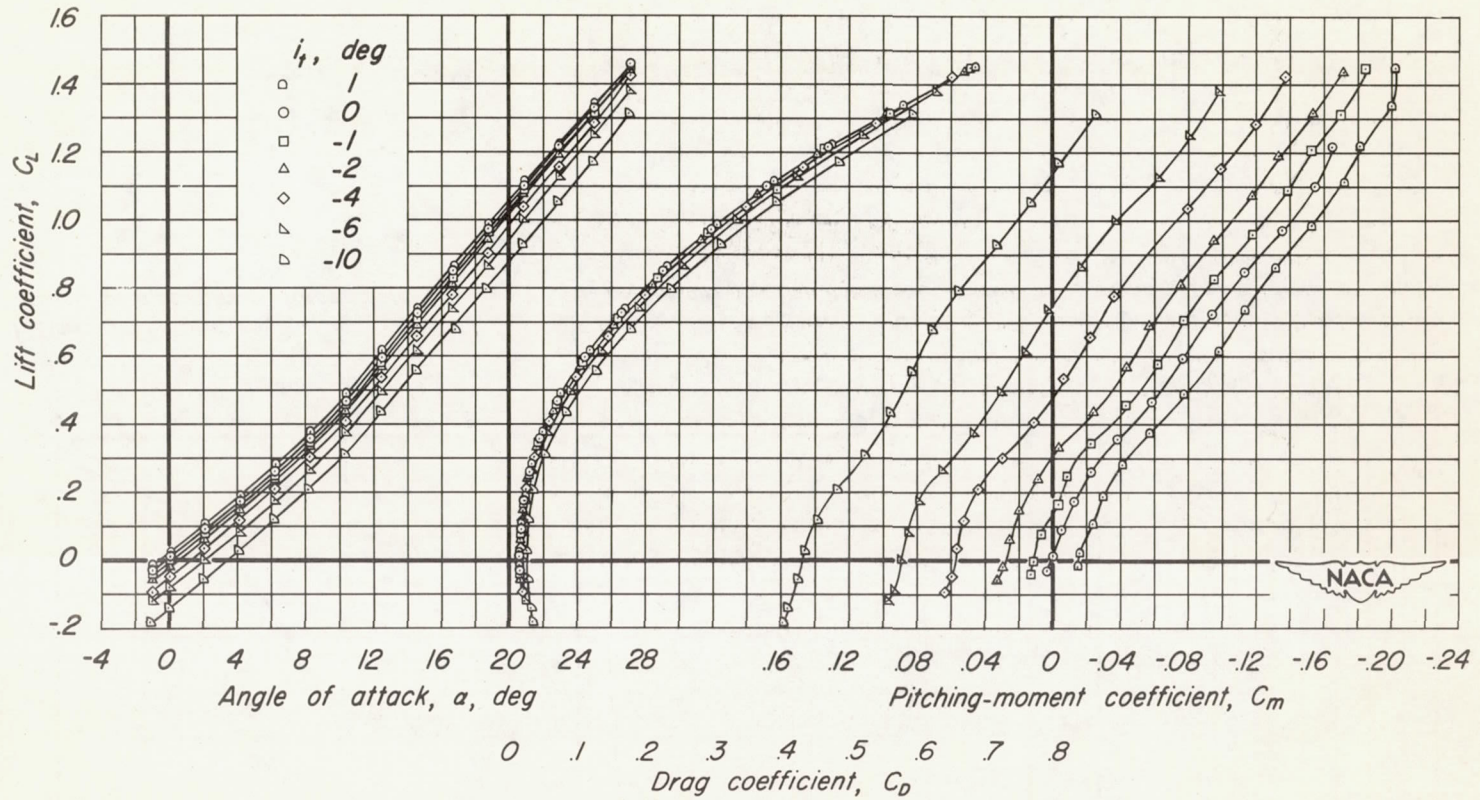
(a) δ_f , $0°$

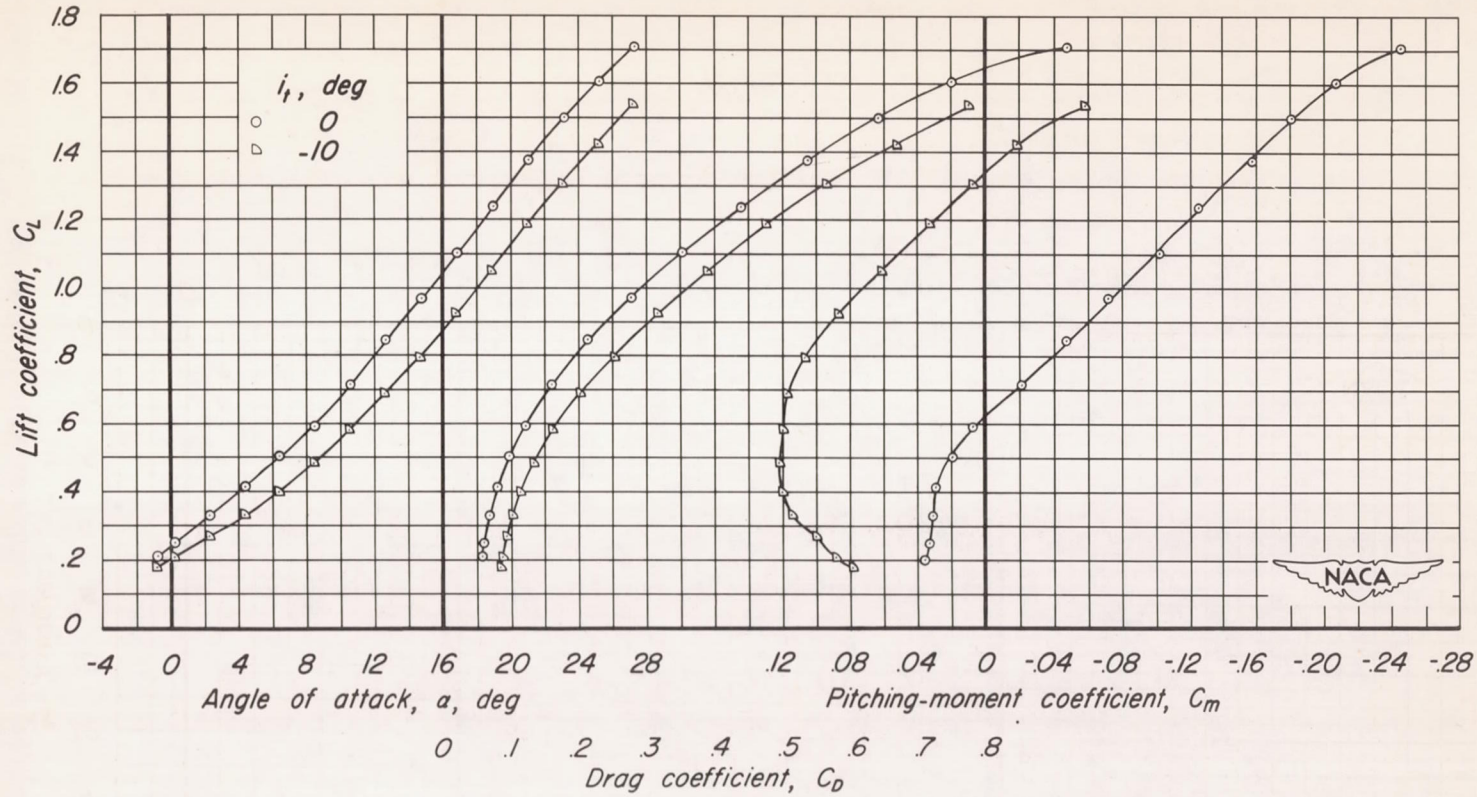Figure 7.- Longitudinal characteristics of the model with the horizontal tail in the low position. $\frac{z}{b/2}$, 0.
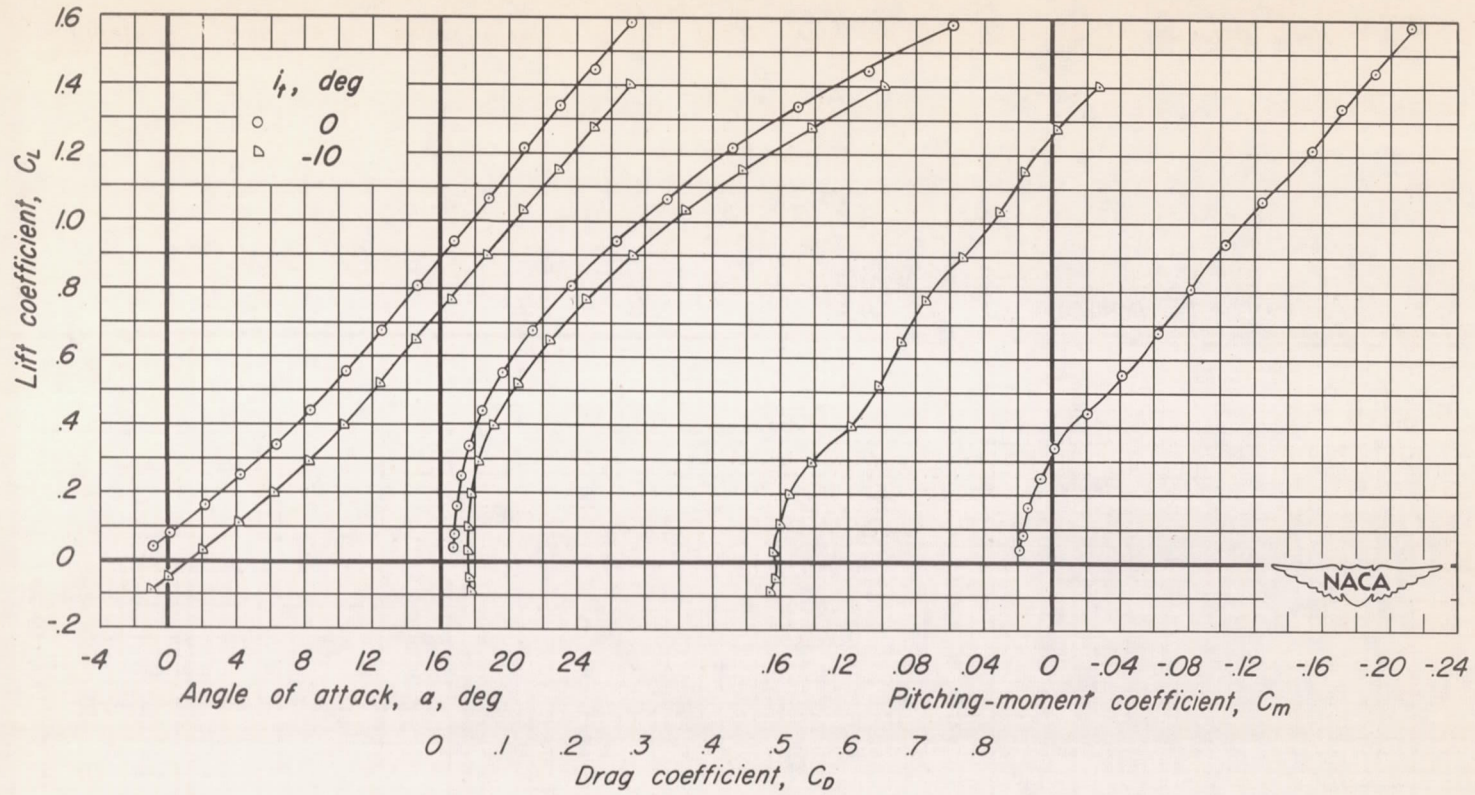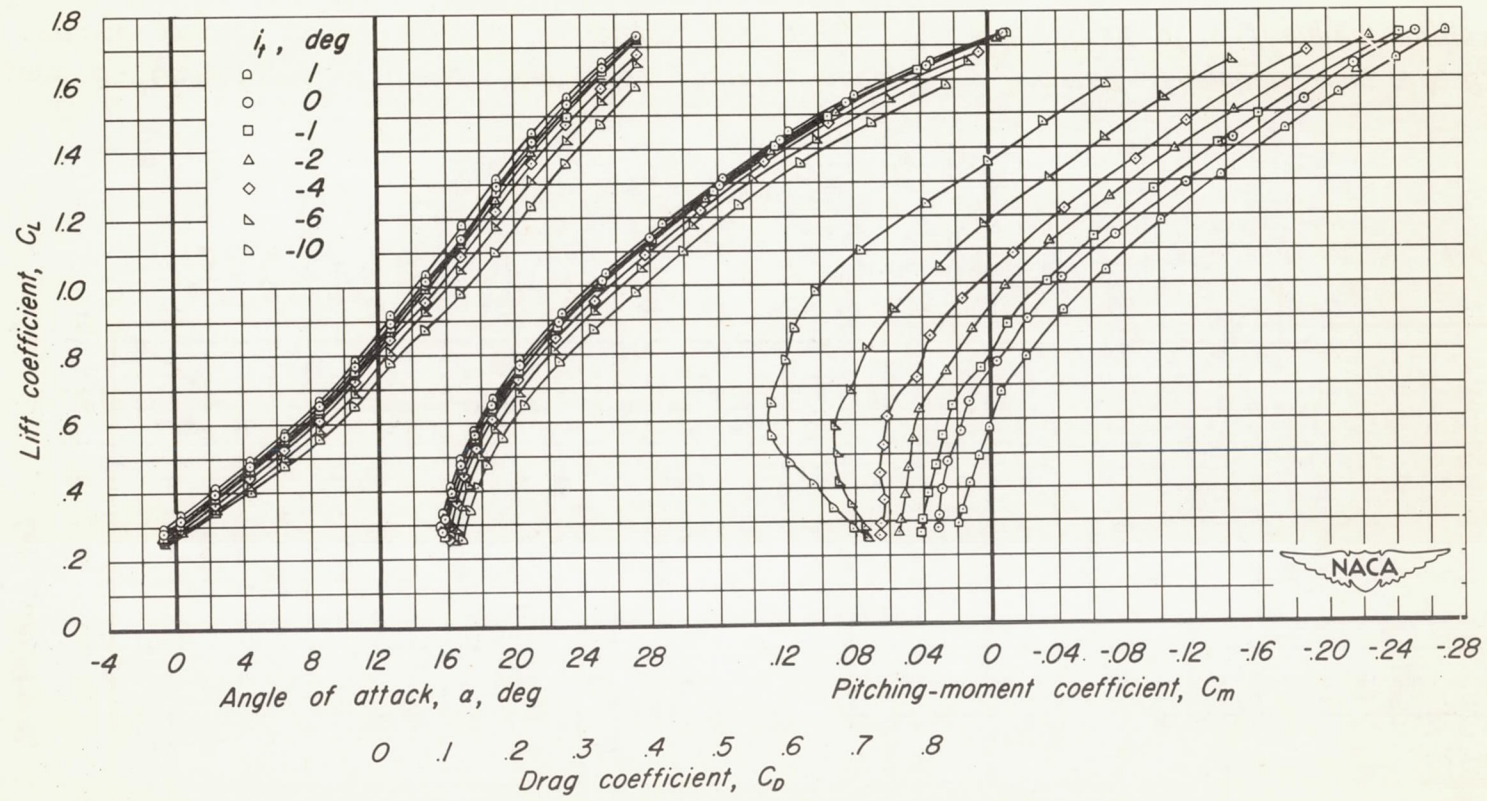
(b) δ_f, 10°

Figure 7.- Continued.

(c) δ_f, 20°

Figure 7.- Continued.

(d) δ_f, 30°

Figure 7.- Continued.

i_t , deg
○ 1
○ 0
□ -1
△ -2
◇ -4
◁ -6
▷ -10

Lift coefficient, C_L

Angle of attack, a, deg

Pitching-moment coefficient, C_m
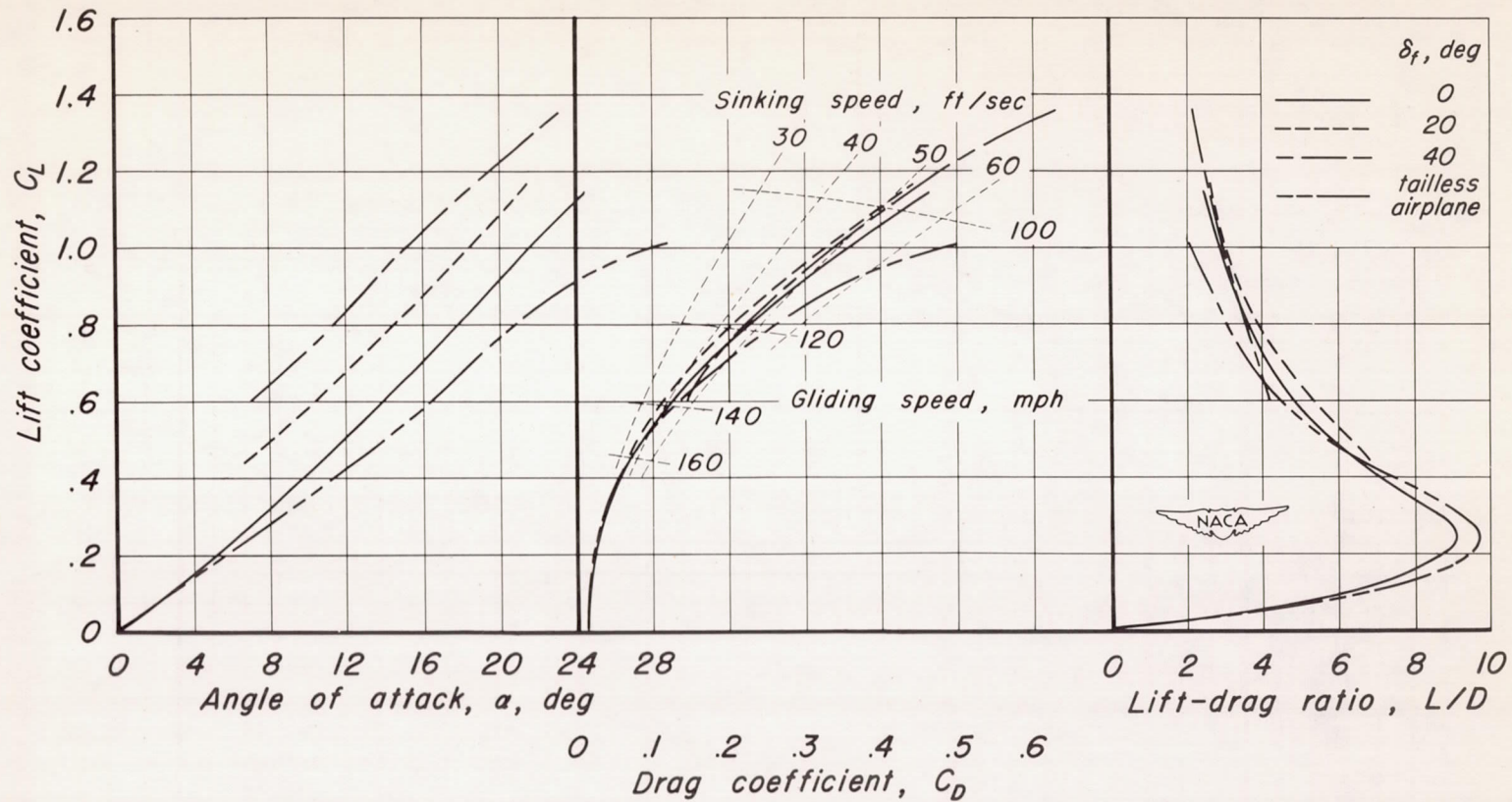
Drag coefficient, C_D
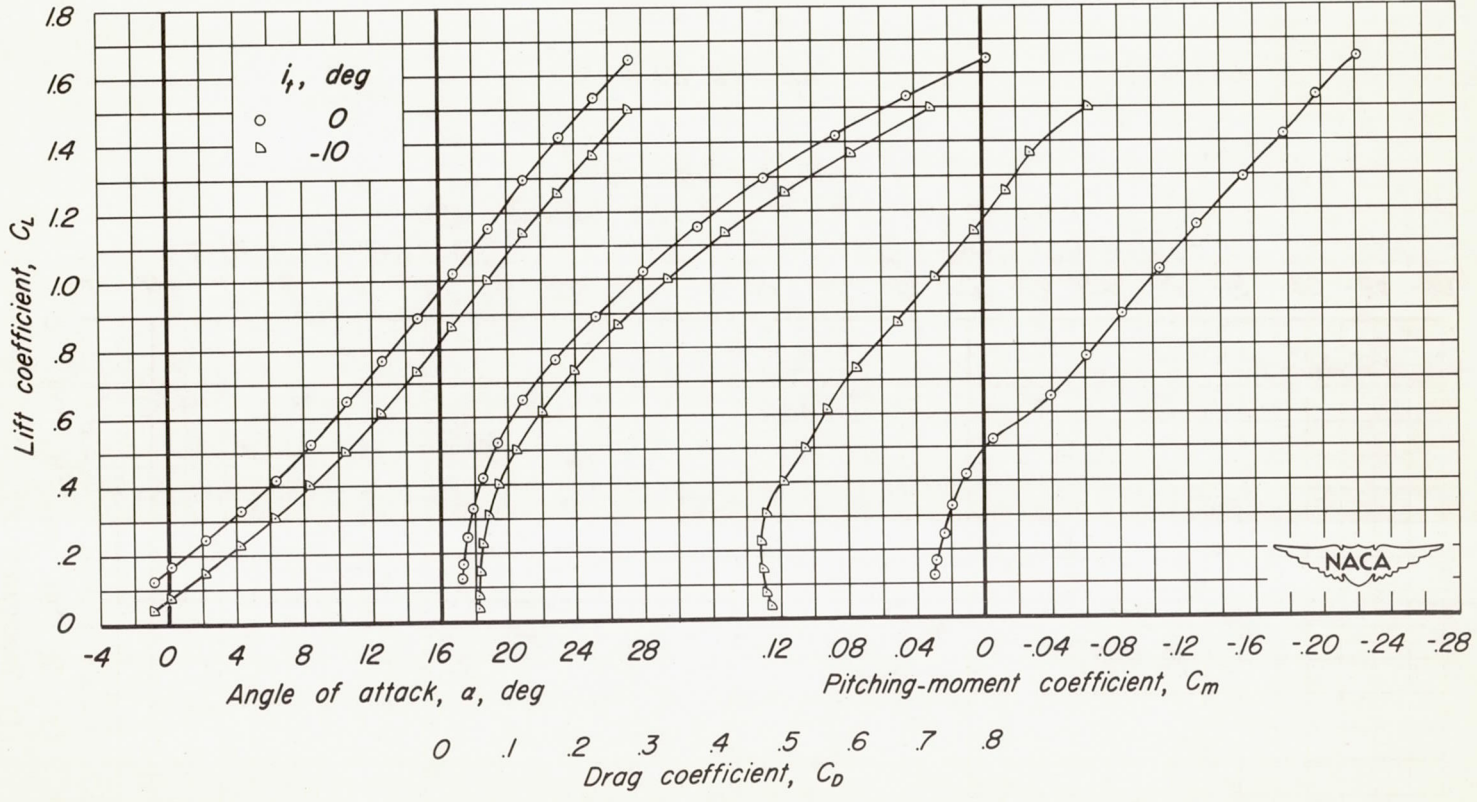
(e) δ_f , 40°

Figure 7.- Concluded.

Figure 8.- Comparison of the lift and drag characteristics of a trimmed, triangular-wing (A, 2.0) airplane having an all-movable horizontal tail ($\frac{z}{b/2}$, 0.) with those of a trimmed, tailless, triangular-wing (A, 2.3) airplane. W/S, 30 pounds per square foot.
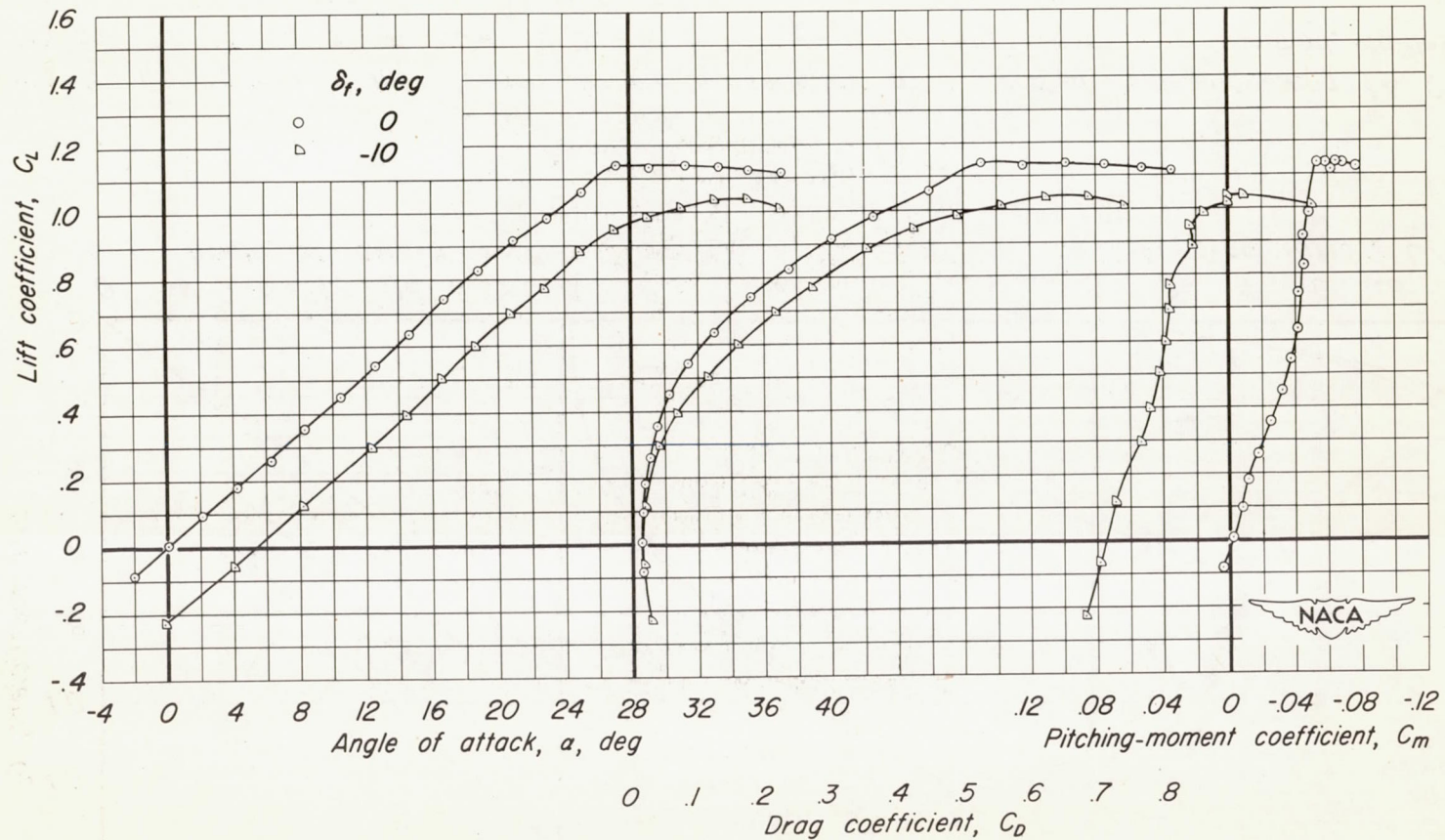
Figure 9.- Aerodynamic characteristics of a tailless, triangular-wing airplane. A, 2.3.

Movement of the vortex
with increasing angle
of attack.

Path of travel of vortex
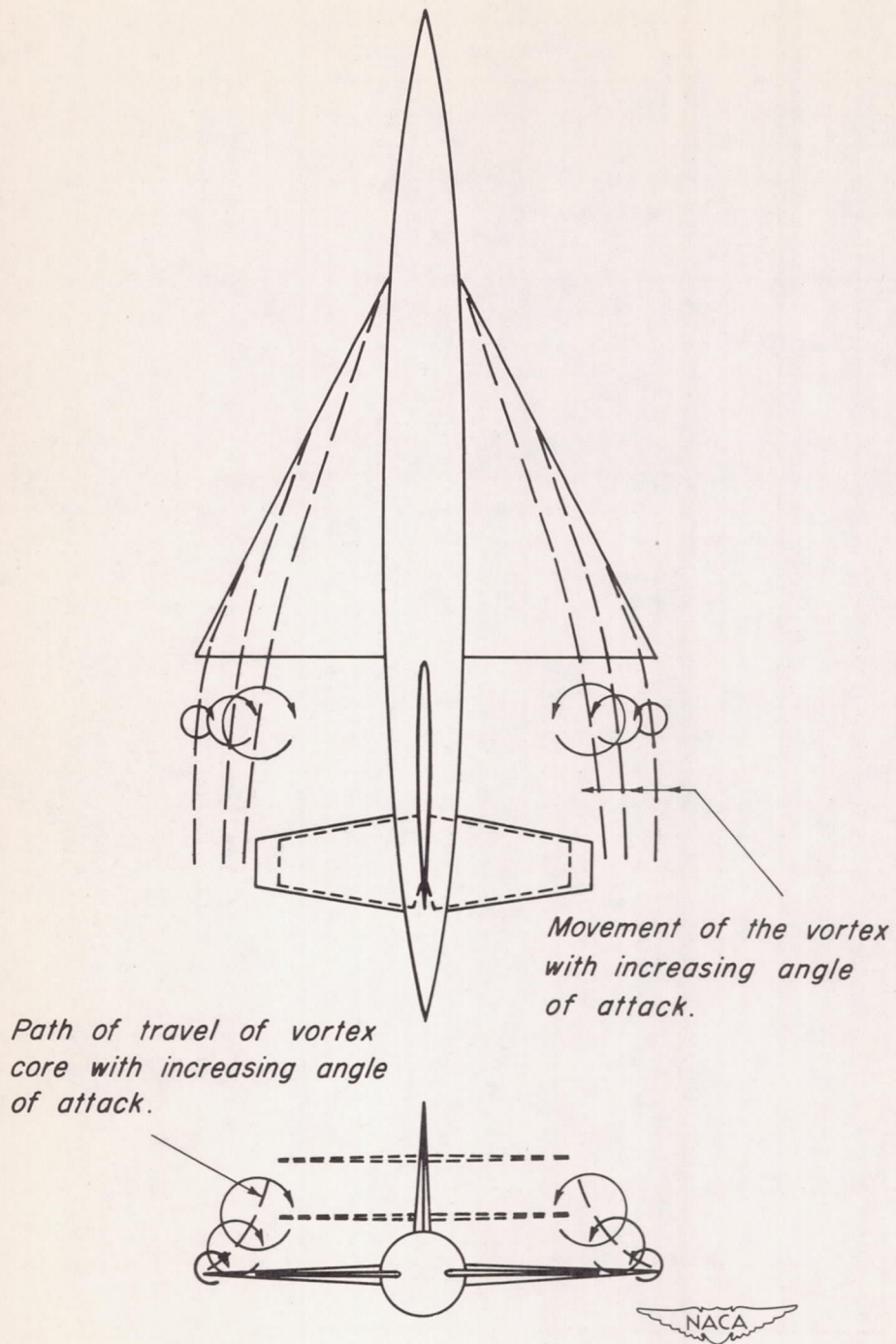core with increasing angle
of attack.

Figure 10.- Influence of the separation vortices on the
downwash at the horizontal tail.